JAM CM Journal of Applied Mathematics and Computational Mechanics 2024, 23(3), 118-129
www.amcm.pcz.pl p-ISSN 2299-9965
DOI: 10.17512/jamcm.2024.3.11 e-ISSN 2353-0588

# THE LOAD ON THE SUPPORTING STRUCTURE OF THE GANTRY CRANE DURING TRAVEL ALONG THE CRANE TRACK

***Ján Vavro, Ján Vavro jr., Ľuboš Marček, Jana Kuricová***

*Faculty of Industrial Technologies in Púchov, Alexander Dubček University of Trenčín Púchov, Slovakia*
*jan.vavro@tnuni.sk, jan.vavro.jr@tnuni.sk, lubos.marcek@tnuni.sk, jana.kuricová@tnuni.sk*

Received: 10 June 2024; Accepted: 9 September 2024

**Abstract.** The paper presents the analysis of the gantry crane loading when travelling along the crane track, using a 3D model, which was used for the analysis of the gantry crane support construction under the loading. The gantry crane is designed to remove dirt that is in front of the turbine under the water surface. The gantry crane, which travels along a track, was subjected to investigation, and the directional and vertical unevenness at the time of travelling were determined and are given in graphic form in [mm] for A track and B track with a total track length of 450 m. Based on the knowledge of the unevenness of the rail track, four random functional dependencies, defining the unevenness of the individual rails, were used as input variables for the kinematic excitation of the individual wheels of the gantry crane. The stress analysis was performed for a travel speed of 30 m/min and a lift of 10 t. The results of the stress analysis are presented in graphic form. In addition to the operating load, the inherent frequencies of the crane construction are also an important factor, which, along with the excitation frequency, can affect the overall global loss of the crane stability. The stability of the crane during its operation is closely related to the load applied to the crane supporting construction. In computer simulations, stability is expressed by a critical force ($F_{crit.}$) and when it is exceeded, local or global stability will be lost. In the paper, the first 10 eigenfrequencies of the crane are given in table form, and the first three eigenshapes are shown in graphic form. The overall loss of crane stability, which is expressed by the critical force ($F_{crit.}$), is also shown in graphic form.

***MSC 2010:*** *37N30, 68U20*
***Keywords:*** *loading, virtual model, stress analysis, 3D model, critical force*

## 1. Introduction

The solution of the real practice problems often involves solving the complex systems, including differential, integral, as well as algebraic equations. In the most cases, it is impossible to obtain analytical solutions, and therefore, the designers utilise the specialised numerical processing methods with the use of modern computational technology.

Modern computational methods depend on the creation of a virtual model with subsequent simulation of the operating process of a given system, without which the work of the designer is unthinkable and impossible in relation to solving the complex problems, the solution of which often brings significant economic benefits.

Based on the requirements of the practice, the main task of a designer is to design and modify the parameters of the proposed device appropriately and precisely, taking into account the other important and specific features of the device, such as its mass, shape, geometry, or some other dynamic properties. The main objective is usually to be able to save material and to find the best solution in terms of material utilization and the suitable shape of the structure.

Nowadays, the increased requirements for material saving, durability, reliability of products and machinery require some new approaches in solving the challenges of the engineering practice. With the help of the adequate and suitable computational programs, a precise, quick and efficient study can be made because, in a greater or lesser extent, this study can be important material from the aspect of the influence of the static and dynamic characteristics of the machine.

The determination of the eigenfrequencies [1-4], and the corresponding eigen-shapes of the investigated mechanical system are predominantly important for engineers when they evaluate the behaviour of a modelled object that is subjected to time-varying forces with the significant harmonic components. This is primarily concerned with the fact that the significant excitation frequencies and the eigen-frequencies of the system should not be the same and they should exhibit sufficient mutual distance. Otherwise, the eigenoscillations can be built up that are closely connected with the so-called resonance phenomenon, which is unacceptable during the device operation because it is often accompanied by the malfunction and sub-sequent failure of the construction. In many cases, the safety and reliability of the crane operation depends on its perfect stability. The global stability of the crane as a whole can be described as its ability to withstand moments when it is tipped up during the lifting the loads, as well as its ability to withstand wind forces, the self-weight of the individual elements and aggregates, and dynamic loads which arise due to its movement on an uneven track.

The condition for the stability of the crane is based on the equality (or degree of incline) of the moment of stability ($M_{stab.}$) in relation to the force of the crane gravity, with respect to all the forces that can cause the moment of the tipping up ($M_{tip.}$).

The condition for stability can be expressed: $M_{stab.} \geq M_{tip.}$, where: $M_{stab.}$ – the re-sulting moment of stability, $M_{tip.}$ – the moment of the tipping up, with respect to the external forces.

All the moments are calculated for cranes that move on rails to the axes of contact of the travelling wheels with the rail. In relation to the stability calculation, the most unfavourable load for the crane operation, along with the combination of the other external loads, is selected.

Crane operation may also result in a so-called local loss of stability due to over-loading in some part of the construction. During the computational simulation, the stability is expressed by the critical force ($F_{crit.}$) and when it is exceeded, either local or global loss of stability occurs The stability of the crane was calculated for the most unfavorable external load.

## 2. Crane rail track measurement results (directional and vertical deflections)

Track unevenness or irregularities are usually divided into vertical and transverse. The above-mentioned track unevenness results in excitation for the vertical movement – vertical unevenness or irregularities and transverse elevation of the track rails, usually in the form of angular shifts (this represents one of the excitation inputs for the transverse travel). In relation to the transverse unevenness or irregularities, the crosswise deflections of the track centreline and the rail gauge deflection are usually considered. This means that the four excitation random functions (left and right rail in both transverse and vertical directions) result in four, which are related to certain types of oscillatory motion of the gantry crane (vehicle).

The rail track is a complex dynamic system that changes its shape when it is subjected to variable movement loads that are caused by the double wheels of the crane. The change in the shape of the track is random because its flexure is influenced by the following factors:

- the vertical flexuosity of the rails,
- the elastic pads between the rail flange and the foundation,
- the quality of the ballast bed, especially the condition of how the individual sleepers are fastened,
- defects in the load-bearing capacity of the railway construction (structure),
- the dynamic characteristics of the gantry crane which moves on the rail.

In this case, since the rail track is embedded in concrete, the dynamic properties of the gantry crane are going to be only considered.

The experimental investigation of the rail unevenness or irregularities is based on geodetic methods. The vertical deflections for the rail track are shown graphically in Figures 1 and 2 shows the directional deflections of the rail track.

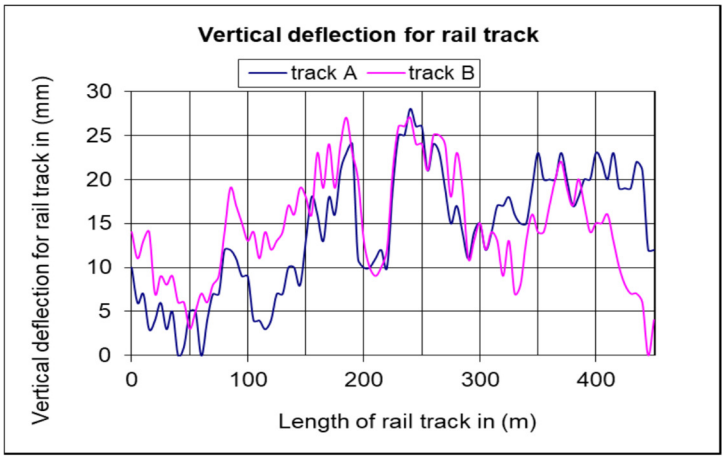


Fig. 1. The vertical unevenness for the rails – $u_{yL}^{(1)}$ (rail designated as A) and $u_{yP}^{(1)}$ (rail designated as B)

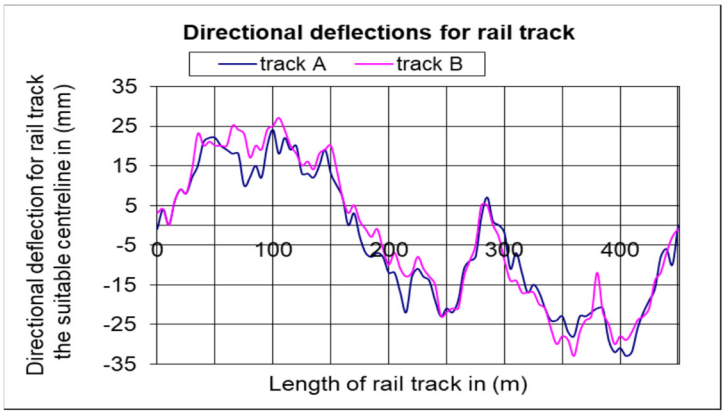


Fig. 2. The directional unevenness for the rails – $u_{xL}^{(1)}$ (rail designated as A) and $u_{xP}^{(1)}$ (rail designated as B)

## 3. Computer verification of the crane computational model

The gantry crane (Fig. 3) is designed to remove dirt that is in front of the turbine under the water surface. The gantry crane was made of steel grade 10 373, currently its equivalent is steel 11 373.

The required mechanical properties of the given steel are: $R_{e\,min} = 235$ MPa (yield point), $R_m = 340\text{-}470$ MPa (tensile strength), $\sigma_{all} = 210$ MPa (allowable stress).

Fig. 3. The view of the portal gantry crane

The operating mode of the gantry crane (operating cycle) can be described in these steps:

- movement of the crane along the track at the specified degree of travelling speed without any load,

- lifting of the load,
- movement of the crane along the track at the specified travelling speed with load.

The following parameters are used as input parameters for the computational model:

- Young's modulus of elasticity: $E = 210$ GPa,
- Poisson's number: $\mu = 0.3$,
- the density of the material: $\rho = 7800$ kg/m$^3$.

External loading:

- load to be lifted: $Q = 32$ t, 10 t, 5 t,
- weight of the crane and individual aggregates according to the technical documentation,
- kinematic excitation resulting from the unevenness of the rail track.

On the basis of the known unevenness of the rail track, four random functional dependencies (Figs. 1 and 2), which define the unevenness of individual rails in dependency on the track, are used as input variables for the kinematic excitation of the individual wheels of the gantry crane [2, 3, 5-8], where:

$v$ – gantry crane speed: $v = 30$ m/min,

$L$ – wheel base 5.2 m,

$u_{xL}^{(1)}$ – unevenness of the left rail in transverse direction for the front axle,

$u_{yL}^{(1)}$ – unevenness of the left rail in vertical direction for the front axle,

$u_{xP}^{(1)}$ – unevenness of the right rail in transverse direction for the front axle,

$u_{yP}^{(1)}$ – unevenness of the right rail in vertical direction for the front axle,

$u_{xL}^{(2)}$ – unevenness of the left rail in transverse direction for the rear axle, i.e.

$$u_{xL}^{(2)}(t) = u_{xL}^{(1)}\left(t - \frac{L}{v}\right),$$

$u_{yL}^{(2)}$ – unevenness of the left rail in vertical direction for the rear axle, i.e.

$$u_{yL}^{(2)}(t) = u_{yL}^{(1)}\left(t - \frac{L}{v}\right),$$

$u_{xP}^{(2)}$ – unevenness of the right rail in transverse direction for the rear axle, i.e.

$$u_{xP}^{(2)}(t) = u_{xP}^{(1)}\left(t - \frac{L}{v}\right),$$

$u_{yP}^{(2)}$ – unevenness of the right rail in vertical direction for the rear axle, i.e.

$$u_{yP}^{(2)}(t) = u_{yP}^{(1)}\left(t - \frac{L}{v}\right).$$

In reference to the technical documentation, a finite element 3D model of the gantry crane construction was created (Figs. 4 and 5) for which the eigenfrequencies

and the stability loss were calculated [3, 6, 7, 10]. In our work, we used the standard STN EN 1090-2+A1.

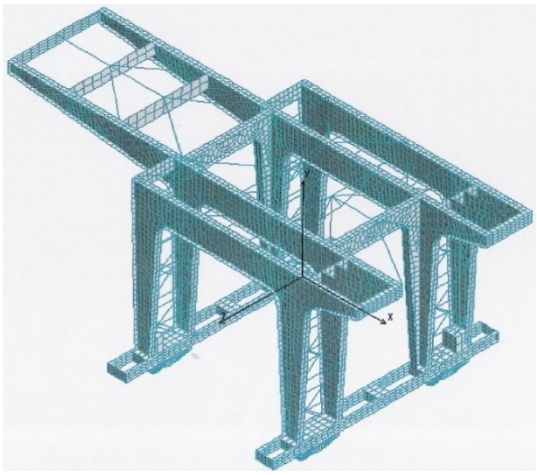

Fig. 4. The finite element model of the gantry crane frame

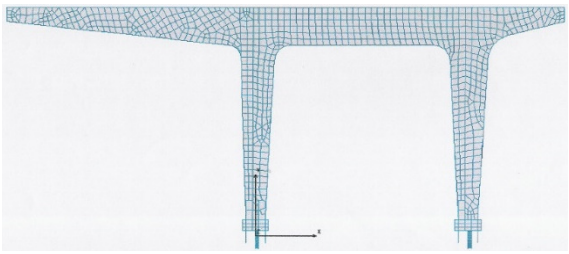

Fig. 5. The view of the finite element model in the direction of x-axis

## 4. Results for loading and stability loss for gantry crane supporting construction

Numerical analysis was performed in the Cosmos Motion 2.92 program environment, which enables finite element analysis of the computational model in motion, under specified boundary conditions.

In Figure 6, there is the stress distribution for the crane construction with respect to the loading relating to its own crane weight and the weight of the individual aggregates (according to technical drawings), the lifted load of 10 t and the travelling speed of 30 m/min. This is the maximum value of stress that is allowed to be reached during the operating process of the gantry crane. The specified value of stress for the construction is not going to be beyond the yield stress $\sigma_{all}$ = 210 MPa and in relation to calculated stress ($\sigma_{cal.}$), the loading condition can be expressed as $\sigma_{all} \geq \sigma_{cal.}$.

In the case of investigated loading for gantry crane, the value of 210 MPa is higher than the calculated value, which was 185.69 MPa, and it means that the gantry

crane construction is suitable for the loading during the operating process of the crane. The magnitude of the load is affected by the vertical and transverse unevenness of the track.

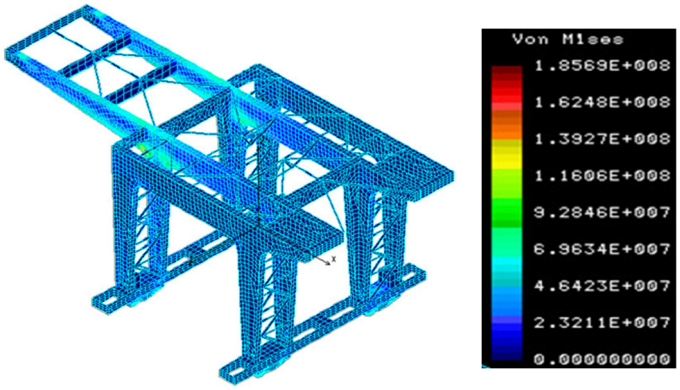


Fig. 6. The maximum stress distribution in track point of 100 m and lift of 10 t in [Pa]

In Figure 7, there is the stress distribution for the crane supporting construction with respect to the loading relating to the own crane weight and the weight of the individual aggregates (according to technical drawings) for the lifted load of 32 t and the specified travelling speed on the rail track. This is the minimum value of stress that is reached during the operating process of the gantry crane. The calculated stress value for load 10 t is greater because it acts on the longer arm on the left (see Fig. 5). A load of 32 t acts on the shorter arm to the right.

The specified value of stress for the construction was not beyond the yield stress $\sigma_{all}$ = 210 MPa and in relation to calculated stress ($\sigma_{cal.}$), the loading condition can be expressed as $\sigma_{all} \geq \sigma_{cal.}$.

Relating to this case, there is: 210 MPa is ≥142.3 MPa, and it means that the gantry crane support construction is suitable for the given load of crane operation. The magnitude of the load is influenced by the vertical and transverse unevenness of the track.

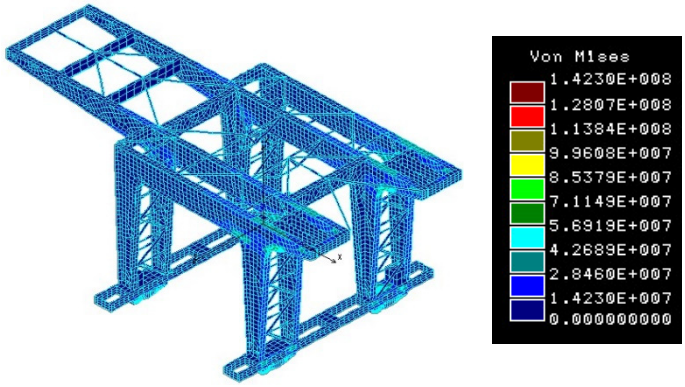


Fig. 7. The minimum stress distribution for lift of 32 t in [Pa]

The stability of the crane (Fig. 8) was performed for a lifted load of 10 t, a crane travelling speed of 30 m/min and for specified unevenness of the rail track in the vertical and transverse direction at a point in the track of 100 m (stress distribution Fig. 6). An overall loss of stability occurs when an overloading force of 11,764 N is applied when the travelling wheel loses contact with the rail.

For the stress distribution 172 MPa, the overall loss of the stability can occur at an overloading force of 16,839 N during the loss of contact of the travelling wheel with the rail.

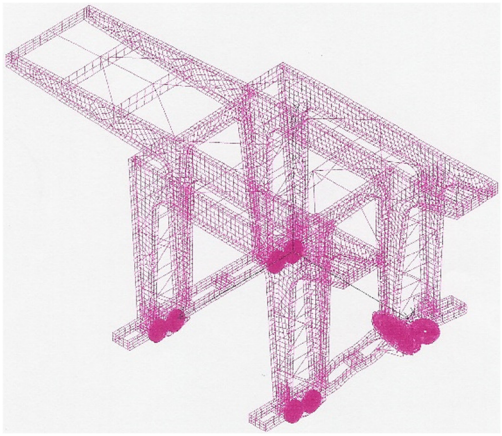

Fig. 8. The global loss of crane stability in track point of 100 m and lift of 10 t

## 5. Modal analysis of a gantry crane

The solution of homogeneous differential equation (1) with homogeneous boundary conditions is very important for solving the linear dynamics problems [1, 3, 7, 10, 11]. From the aspect of mechanics for constructions, the condition of natural or free vibrations has to be taken into account

$$\mathbf{M} \cdot \ddot{\mathbf{u}}(t) + \mathbf{K} \cdot \mathbf{u}(t) = \mathbf{0} \tag{1}$$

where: **M** – matrix of weight, **K –** matrix of stiffness, **u** – vector of shifts, **ü** – vector of accelerations.
The solution and relation can be expressed in the form:

$$\mathbf{u}(t) = \mathbf{y} \cdot \sin(\omega \cdot t). \tag{2}$$

Calculation of **ü** and its application (1) can result in the basic equation for solution of undamped free vibrations:

$$\left(-\omega^2 \cdot \mathbf{M} + \mathbf{K}\right) \cdot \mathbf{y} = \mathbf{0}. \tag{3}$$

From the aspect of Mathematics, equation (3) represents an eigenvalues problem for the **M** and **K** matrices. It is clear that in order to gain a non-trivial solution of equation (3), it is necessary to fulfill the condition:

$$\det(\mathbf{K} - \omega^2 \cdot \mathbf{M}) = 0 \tag{4}$$

If the measure of **M** and **K** matrices is *n x n*, then the *n* of angular eigenfrequencies ($\omega_i$) and the *n* of eigenshapes ($y_i$) can be calculated. The eigenfrequencies can be ordered on the measure of magnitude: $\omega_1 \leq \omega_2 \leq \ldots \leq \omega_n$. All of the solutions which are based on equation (3) can be expressed in a single equation by alignment of the $y_i$ vectors into a modal matrix (**V**) ($y_i$ forms a column of the modal matrix) and by alignment of the squares of the eigenfrequencies into a diagonal spectral matrix (**Ω**) and then:

$$(\mathbf{K} - \Omega^2 \cdot \mathbf{M}) \cdot \mathbf{V} = \mathbf{0} \tag{5}$$

The first three eigenfrequency shapes of the gantry crane are shown in Figures 9-11 and in the first ten eigenfrequencies of the gantry crane construction can be seen in Table 1.

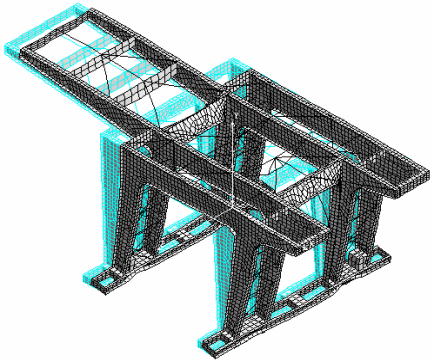

Fig. 9. The first shape of the eigenfrequency

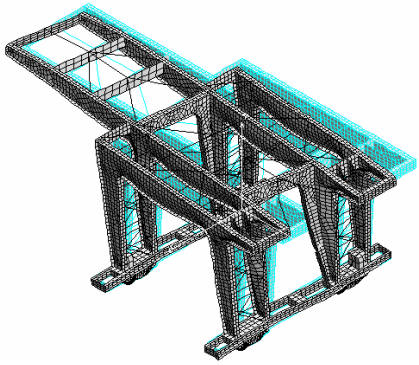

Fig. 10. The second shape of the eigenfrequency

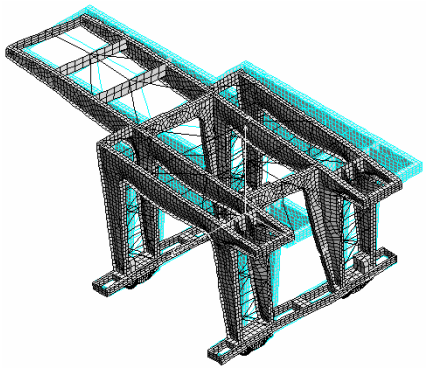

Fig. 11. The third shape of the eigenfrequency

Table 1. The first ten eignefrequencies for gantry crane support construction (frame)

| Number frequency | Frequency [rad/sec] | Frequency [Hz] | Period (Time interval) [s] |
|---|---|---|---|
| 1 | 0.4427279E+02 | 0.7046233E+01 | 0.1419198E+00 |
| 2 | 0.5122712E+02 | 0.8153050E+01 | 0.1226535E+00 |
| 3 | 0.6001209E+02 | 0.9551221E+01 | 0.1046987E+00 |
| 4 | 0.8300188E+02 | 0.1321016E+02 | 0.7569931E-01 |
| 5 | 0.8918526E+02 | 0.1419428E+02 | 0.7045094E-01 |
| 6 | 0.9769244E+02 | 0.1554823E+02 | 0.6431598E-01 |
| 7 | 0.1012056E+03 | 0.1610738E+02 | 0.6208335E-01 |
| 8 | 0.1037301E+03 | 0.1650916E+02 | 0.6057245E-01 |
| 9 | 0.1044198E+03 | 0.1661892E+02 | 0.6017238E-01 |
| 10 | 0.1103911E+03 | 0.1756929E+02 | 0.5691749E-01 |

## 6. Conclusion

The reliable and safe operating process of a gantry crane depends on several factors. The loading represents one of the main factors that have to be taken into account in relation to the reliability of the gantry crane. The given loading is not allowed to exceed a certain value of the allowable load on the construction when it is in operating mode. The given loading condition is expressed in the form of $\sigma_{all} \geq \sigma_{cal.}$, where $\sigma_{all}$ represents the allowable stress of a given material and $\sigma_{cal.}$ is the calculated stress for the construction in relation to a given specific load.

The gantry crane loading ranges from 142.3 MPa to 185.69 MPa. The gantry crane supporting construction is suitable for the reliable operation of the given crane. The maximum load of 185.69 MPa is less than the allowable load of 210 MPa.

The measure of the load is also affected by the vertical and transverse unevenness of the track.

Stability is the second important factor in relation to the gantry crane during the operating process. The given stability is closely related to the load on the crane structure. The loss of stability is possible in the case if the external load was increased by the critical force ($F_{crit.}$) = 0.039701. In the Figure 6, the external force ($F_{ext.}$) is 0.039701*296,318 = 11,764 N for a track point of 100 m and a lift of 10 t. The stability of the crane depends on the external loading as well as on the roughness of the rail track. In the case of 172 MPa stress distrbution, there is the loss of stability when the value of $F_{crit.}$ is exceeded (see: $F_{crit.}$ = 0.0455111*$F_{ext.}$ = 0.455111*370,000 = = 16,839 N).

The measure of stability can be increased significantly if the travelling speed is limited to 15 m/min and if two different operating activities are not performed simultaneously, i.e. lifting and travelling at the same time. The stability of the gantry crane is also based on the eigenfrequency of the crane. The modal analysis shows that the first eigenfrequency of the crane has the most significant or the greatest effect.

## Acknowledgement

This work was supported by the Slovak Grant Agency – project KEGA 011TnUAD-4/2024.

## References

[1] Dižo, J., Harušinec, J., & Blatnický, M. (2018). Computation of modal properties of two types of freight wagon bogie frames using the finite element method. *Manufacturing Technology*, *18*, 2, 208-214.

[2] Klimenda, F., Svoboda, M., Rychlikova, L., & Petrenko, A. (2015). Investigation of vertical vibration of a vehicle vodel driving through a horizontal curve. *Manufacturing Technology*, *15*, 143-148.

[3] Vavro, J., & Vavro, J., jr., (2019). *Aplikácia výpočtových a experimentálnych metód v gumárenskom priemysle*. ASSA spol. s.r.o., Púchov, 120 p.

[4] Vavro, J., Vavro, J., jr., Kianicová, M., Vavrová, A., Pecušová, B., (2019). Numerical modal analysis of the turbo-jet engine rotor blades. *Manufacturing Technology*, *19*, 6, 1067-1070.

[5] Loulová, M., Suchánek, A., & Harušinec, J. (2017). Evaluation of the parameters affecting passenger riding comfort of a rail vehicle. *Manufacturing Technology*, *17*, 2, 224-231.

[6] Saga, M., Sapietová, A., Vaško, M., Dekýš, V., Kuric, i., Čuboňová, N., Krajčovič, M., & Dulina, Ľ. (2015). *Chosen Applications of Computer Modelling in Mechanical Engineering*. Pearson, 230.

[7] Saga, M., Sapietová, A., Žmindák, M., & Dekýš, V. (2016). *Methods for Analysis and Synthesis of Dynamic Systems in Mechanical Engineering*. Pearson, 290.

[8] Svoboda, M., Chalupa, M., Černohlávek, V., Švásta, A., Meller, A., & Schmid, V. (2023). Measuring the quality of driving characteristics of a passenger car with passive shock absorbers. *Manufacturing Technology*, *23*, 1, DOI: 10.21062/mft.2023.023.

[9] Tomsovsky, L., Lopot, F., & Jelen, K. (2022). Kinematic analysis of the tram-pedestrian collision – a preliminary case study. *Manufacturing Technology*, *22*, 1, DOI: 10.21062/mft.2022.007.

[10] Schweighardt, A., Vehovszky, B., & Feszty, D. (2020). Modal analysis of the tubular space frame of a formula student race car. *Manufacturing Technology*, *20*, 1, DOI: 10.21062/mft.2020.013.

[11] Vavro, J., & Vavro, J., jr., (2023). *Analysis and Synthesis of Planar Mechanisms*. ISBN 978-80-908447-1-1, 146 p.